2011

FABRICATION OF MWCNT BASED GAS SENSOR USING SITE-SELECTIVE GROWTH OF NANOTUBES ON GOLD PATTERNED SILICON OXIDE SUBSTRATE

Srikanth Durgamahanty
University of Kentucky, sdu222@uky.edu

ABSTRACT OF THESIS

FABRICATION OF MWCNT BASED GAS SENSOR USING SITE-SELECTIVE GROWTH OF NANOTUBES ON GOLD PATTERNED SILICON OXIDE SUBSTRATE

Growth confinement techniques for multi walled carbon nanotubes on Au/SiO_2 surfaces was studied and incorporated into a gas sensor design. A device framework was conceived and a sensor was built to achieve this structure. The fabrication results were analyzed using scanning electron microscopy which confirmed the achievement of highly site-selective growth of carbon nanotubes, exclusively between the interdigitated electrodes. The sensor was then evaluated for its capacitance and conductance response when exposed to NO_2 gas. Variation in sensitivities with frequency and flow rate were analyzed. A mathematical model was derived for such a device structure and the predictions of the model were compared with experimental results.

KEYWORDS: MWCNTs, Gas, Sensor, Growth, Confinement.

Srikanth Durgamahanty

04 March, 2011

FABRICATION OF MWCNT BASED GAS SENSOR USING SITE-SELECTIVE GROWTH OF NANOTUBES ON GOLD PATTERNED SILICON OXIDE SUBSTRATE

By

Srikanth Durgamahanty

Dr. Vijay Singh

Director of Thesis

Dr. Stephen Gedney

Director of Graduate Studies

04 March, 2011

RULES FOR THE USE OF THESES

Unpublished theses submitted for the Master's degree and deposited in the University of Kentucky Library are as a rule open for inspection, but are to be used only with due regard to the rights of the authors. Bibliographical references may be noted, but quotations or summaries of parts may be published only with the permission of the author, and with the usual scholarly acknowledgments.

Extensive copying or publication of the thesis in whole or in part also requires the consent of the Dean of the Graduate School of the University of Kentucky.

A library that borrows this thesis for use by its patrons is expected to secure the signature of each user.

Name Date

THESIS

Srikanth Durgamahanty

The Graduate School

University of Kentucky

2011

FABRICATION OF MWCNT BASED GAS SENSOR USING SITE-SELECTIVE GROWTH OF NANOTUBES ON GOLD PATTERNED SILICON OXIDE SUBSTRATE

THESIS

A thesis submitted in partial fulfillment of the requirements for the degree of Master of Science in Electrical Engineering in the College of Engineering at the University of Kentucky

By

Srikanth Durgamahanty

Lexington, Kentucky

Director: Dr. Vijay P Singh, Professor of Electrical and Computer Engineering

Lexington, Kentucky

2011

ACKNOWLEDGEMENTS

I would like to express my sincere thanks and heartfelt gratitude for my academic advisor and thesis chair Dr. Vijay Singh for his guidance and support throughout my thesis. I am very thankful for his constant encouragement and motivation during the thesis. I would like to extend my thanks to Dr. Ingrid St.Omer and Dr. Janet Lumpp for serving on my thesis committee. Their expertise in this subject matter has helped me write a very high quality thesis. I am especially grateful to Dr. Suresh Rajaputra and Raghu Mangu who taught me a lot about carbon nanotubes and their potential applications in sensors. I am greatly indebted for their technical support throughout my thesis. I also like to thank people in my group for their technical assistance and support.

Furthermore I like to thank Dr. Rodney Andrews and Dali Qian at Centre for Applied Energy Research (CAER) for their support for the growth of carbon nanotubes.

I am greatly indebted to my parents and my brother, for they have been my pillar of strength throughout my studies in the USA.

Table of Contents

List of Tables

List of Figures

1. Introduction:

1.1. Gas sensors

Gas sensors have always been an integral part of industrial processes. They provide critical information about the presence and concentration of a desired gas in a process which is crucial for feedback and process control. In addition, they are used to detect gas leaks that can be explosive or toxic. Gas sensors are being extensively used to monitor various gases in our ambient environment to assess the air quality and also to ensure sources of undesirable gases are controlled. Gas sensors are also found in space explorations to study a planet's atmospheric constituents. It is because of these important applications, extensive research is being done on gas sensors and with the advent of nanotechnology there seems to be a lot of potential for gas sensors research.

1.2. Carbon Nanotubes as a gas sensing material

One of the most common gas sensing principles is adsorption of gas molecules on the sensing material. This material can be a gas sensitive polymer, a semiconductor metal oxide or a porous material [1][2] [3]. Since adsorption and desorption is the driving mechanism for these sensors, increasing the surface area of the gas sensing material with the analyte molecules increases the sensing capability. Carbon nanotubes (CNTs), due to their large surface to volume ratio, therefore offer a tremendous potential as a gas sensing material. Also, the techniques used to grow carbon nanotubes, be it arc discharge, laser ablation or CVD, are well established laboratory processes with an excellent control over the yield, at a lower cost. Large surface area and ease of its growth in laboratory conditions therefore makes CNTs a strong candidate for gas sensing applications.

1.3. Conductance and Capacitance based sensors

Carbon nanotubes show a significant change in their electronic properties such as resistance, thermo power and density of states when exposed to certain gases. Since fabrication and calibration of a sensor based on a resistance change is easy to implement, most of the CNT based sensors reported are of resistive type. Moreover, resistance based sensors have a low recovery time and a faster response. On the other hand, sensors that report a change in capacitance or dielectric properties have a slower response and a slower recovery profile [4]. However, capacitance based sensors have a few advantages over their resistive counterpart. Capacitive based CNT sensors can be integrated into an LC circuit, which can be used for remote gas sensing in a sealed chamber [5]. A circular disk type resonator with SWNTs on top of the disk which when exposed to different gases has been shown to give different changes in resonant frequency shift thus demonstrating selectivity [6][7]. The multitude of added advantages, including the ability to sense remotely as well as demonstrated gas selectivity through varying resonance conditions, calls for further studies into capacitive gas sensors in addition to the conventional conductance based sensors. Successful understanding and fabrication of such a device, holds great promise to the field of sensor devices.

1.4. Literature review

Though a number of devices based upon conductance change have been reported, less information has been published regarding sensors working on capacitance change. Every effort has been made to identify and document such related sensors in this section. Snow et al. [4] was one of the first groups to build a sensor that shows a change in capacitance when exposed to volatile organics and low vapor pressure explosives. Their sensor consisted of a thick layer of oxide grown on a degenerately doped silicon wafer. A network of Single walled carbon nanotubes (SWNTs) grown on the oxide layer via chemical vapor deposition (CVD), formed the sensitive material. An interdigitated electrode (IDE) array of Pd patterned on this SWNT network provided one of the contacts while, the heavily doped Si substrate formed the other contact for measurement. When exposed to a gas under an applied AC bias, the fringing electric fields radiating outward from the SWNTs causes a change in net polarization of the adsorbates that is detected as change in final capacitance. For an exposure as low as P/P_0 = 1% of N,N-dimethylformamide (DMF), a capacitance change of 0.93% was shown along with a good stability and a faster response time relative to SWNTs resistors. P_0 is equilibrium vapor pressure at 25^0 C and P is vapor concentration.

Ong et al. [5] fabricated a wireless inductive-capacitive (LC) circuit gas sensor with a MWNT-SiO_2 composite as a sensing layer. An electrically insulating SiO_2 layer coated onto a printed LC circuit board provides the base onto which a gas sensitive MWNT-SiO_2 composite mixture is placed. When exposed to a gas, the complex permittivity ε of the composite material changes resulting in a change in the resonant frequency of the sensor,

which is picked up by a loop antenna. Decent sensitivities of 0.91%, 0.09% and 2% has been achieved for CO_2, O_2 and NH_3 gases respectively.

Suehiro et al. [8] developed an ammonia sensor using a process called dielectrophoresis (DEP). An interdigitated electrode array of chromium (Cr) was patterned on a glass substrate. MWCNTs purchased from a commercial supplier were ultra-sonicated in ethanol and the suspended solution was made to flow over the substrate at a controlled flow rate. Under an applied AC bias of 10V and 100 kHz, some of the MWCNTs were trapped between the electrodes by positive DEP. After a period of time, the process is stopped and ethanol solution was let to evaporate at room temperature. This sensor is then tested for ammonia gas with a lock in amplifier connected to the contact pads of the IDE array. At the end of 5 minutes, a change of 4pF was reported for this device.

Yeow et al. [9] built a highly sensitive humidity sensor using two parallel steel plates separated by a small gap. One of the plates had a thick mat of MWCNTs grown on them. The screws on either of the plates serve as the electrical contacts during measurement. The device is shown to give a change of 3786 % in capacitance for a change of humidity from 70% RH to 80 % RH. This high sensitivity was achieved because of the capillary condensation effect at the carbon nanotubes surface. As vapor condenses at the surface of the CNTs, it converts to water, that has a higher dielectric constant. This results in overall increase in capacitance of the sensor.

Chen et al. [10] fabricated a device for detecting ammonia and formic acid. CNTs were grown in a anodic alumina template (AAO) using acetone pyrolysis. Gold film deposited on the top and bottom surface of the template formed the two electrical contacts. AAO

was partially etched using 10% HF to expose the CNTs inside the template. This device was reported, to output a change of 2% in capacitance for ammonia and 10% for formic acid. Sensitivity is attributed to the change in net polarization caused by the adsorbate at the surface of the CNTs which gives a change in capacitance between the two electrodes.

Almost all of the CNT sensors surveyed rely on changes in conductance or in dielectric constant, from the interactions between the CNT's and the gas molecules. Therefore, the study of these gas-CNT interactions is of utmost importance for conceiving a blue print of the device structure of a CNT based gas sensor.

2. Theory

2.1. Carbon nanotubes

Since their discovery in 1991 by Iijima [11], carbon nanotubes have been investigated by researchers all over the world. Due to their large aspect ratio (length: diameter) these materials are expected to possess additional interesting electronic, mechanical and molecular properties. Belonging to the family of fullerenes, carbon nanotubes can be seen almost as a one dimensional fullerene. Carbon Nanotubes are of two types – Single Walled and Multi Walled. [12]. An SWCNT can be considered as a layer of graphite rolled up into a cylinder with a diameter of several nanometers, and length on the order of microns [13].There are three distinct ways in which a graphene sheet can be rolled into a tube

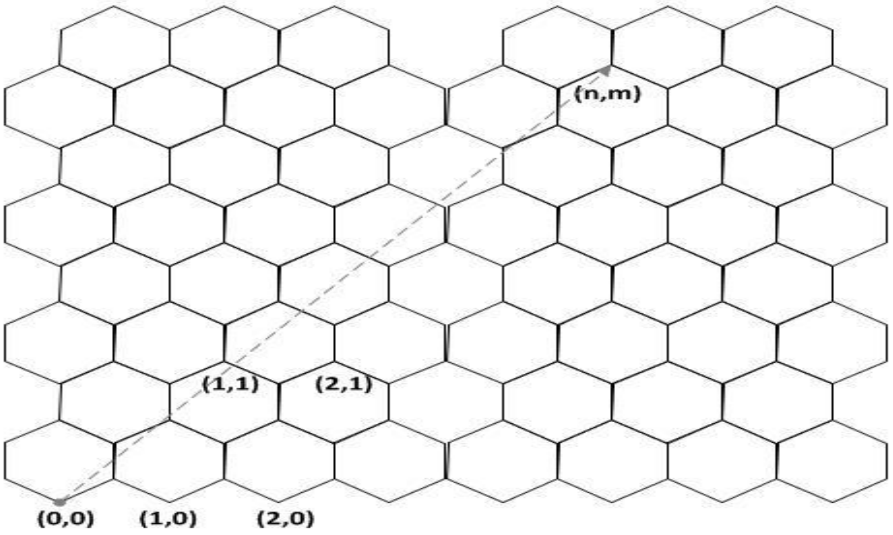

Figure 2.1: A one atom thick layer of graphite with carbon atoms placed at the numbered indices.

The way a graphene sheet is rolled up is specified by a vector (n,m) that defines the structure of a carbon nanotube. Rolling up the layer such that the (0,0) atom superimposes the (n,m) atom produces a carbon nanotube with (n,m) as indices. If n=m then such a tube has an armchair configuration. If m=0 then it's a zigzag configuration. Both armchair and zigzag structures have a high degree of symmetry .The rest of the configurations fall under chiral structure which is the most common form of a carbon nanotube.

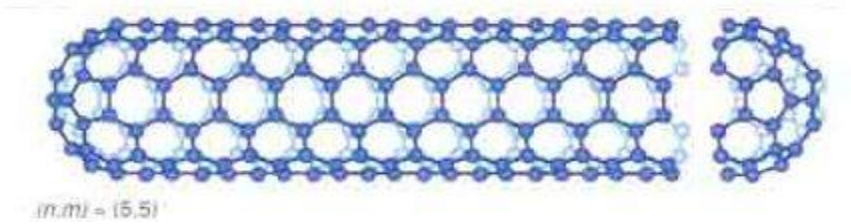

Armchair

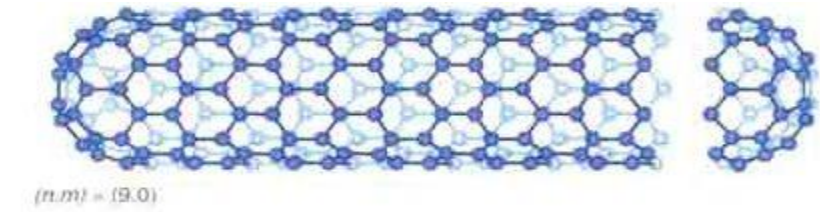

Zigzag

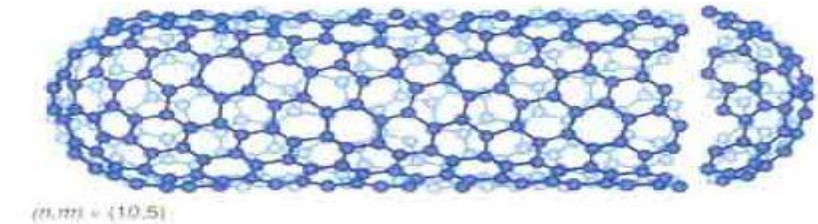

Chiral

Figure 2.2: Configurations of a Single Walled Carbon Nanotube [14]

Multi-walled carbon nanotubes can be considered as multiple layers of graphite rolled in such a manner so as to obtain a tube within a tube structure.

2.2. Carbon nanotubes gas sensing mechanism

Molecule adsorption and its effect on the electronic properties of a carbon nanotube is the primary gas sensing mechanism behind any CNT based gas sensor. Adsorption of NO_2 molecules on SWNTs, studied by first principle calculations, using density functional theory was carried by Peng and Cho [15]. The binding configuration for NO_2 gas molecules on a (10, 0) SWNT is shown in Figure 2.3. The adsorption energy for this binding configuration was reported to be 0.3 eV. Charge transfer studies backed by electron density analysis showed hole doping of the semiconducting SWNT by the NO_2 gas molecules.

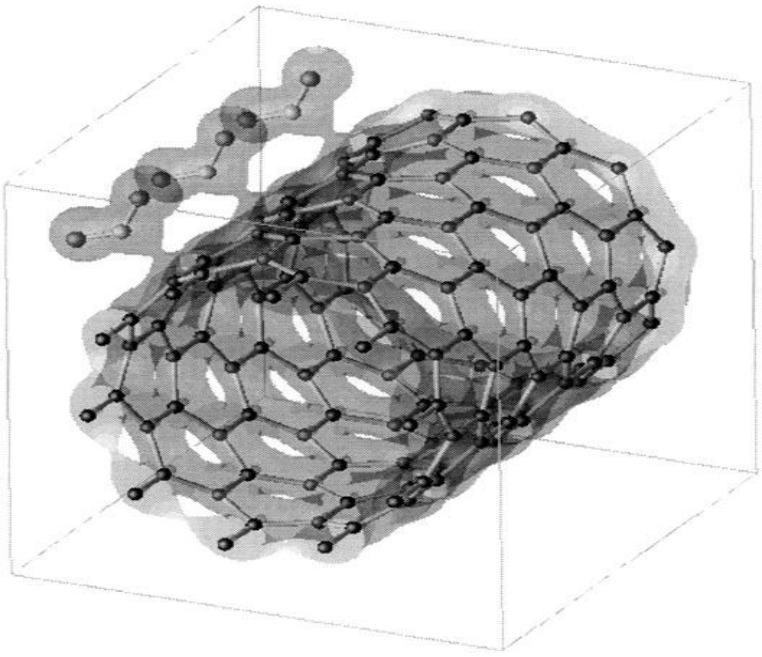

Figure 2.3: Binding configuration of NO_2 molecule on a (10,0) SWNT [15]

Adsorption of various gas molecules on a single nanotube and bundle of nanotubes was investigated by Zhao et al. [16] using the first principles method. Equilibrium tube molecule distance, adsorption energies and charge transfer for these molecules on a (10,0), (17, 0) and (5,5) SWNTs were calculated based on density functional theory. Except for NO_2 and O_2, most of the gas molecules were found to be charge donors with a small charge transfer and weak binding energies (<0.2 eV). NO_2 and O_2 were found to be charge acceptors with large adsorption energies. These calculated results were also consistent with the reported experimental results. [17] [18].

Collins et al. illustrated that parameters such as thermoelectric power and electrical resistance of the SWNTs are extremely sensitive to low concentrations of oxygen. [18].Theoretical studies consistent with experimental results were performed by Jhi et al. on electronic and magnetic properties of oxidized carbon nanotubes, which demonstrated the potential for carbon nanotubes in sensor applications. [19].

Changes in the dielectric properties of the carbon nanotubes as a result of molecular adsorption were studied by Langlet et al. A sensor model was built using a single (17, 0) SWNT with length and radius of 27.36 and 6.75 A^o respectively. A mathematical expression for the local electric field at a position, because of a carbon atom in the nanotube and an admolecule was derived that was used to calculate the interaction energy between the tube and the admolecule, and also to determine the linear dielectric susceptibility of the system formed by the SWNT and the admolecule. The mathematical model is solved to obtain an expression, which shows that the variation in linear dielectric susceptibility with molecular adsorption is proportional to the molecular polarizability of the constituents. Change in permittivity before and after molecular

adsorption for different gas species were calculated using this model. Results of this sensor model showed that the largest molecular polarizability (which corresponds to molecule size) produced the largest change in permittivity ratio. [20]

2.3. Carbon nanotube growth confinement on Au patterned SiO_2/Si substrate

For a capacitive sensor the placement of the sensing dielectric (CNTs in this case), ideally should be between the metal electrodes. This arrangement reduces complications in developing a mathematical model for such a device which is crucial for its understanding. Achieving such a high degree of arrangement, it is essential that the growth of CNTs occur only in the desired area. Such a growth confinement technique has been demonstrated successfully by Cao et al on gold (Au) patterned quartz substrates [21]. In order to understand the nanotubes growth confinement mechanism, it is essential to know the science behind CNT growth on a given substrate. Laser ablation [22], arc discharge [11] and catalytic decomposition of hydrocarbons [23] have been the primary methods for CNT production for a long time. Since growth of nanotubes by catalytic decomposition of hydrocarbons, has been utilized in this study, only the growth mechanism for this technique is discussed in this work.

Carbon nanotube growth can be assumed to be an extension of a process in which graphitic structures grow over metal surfaces at temperatures below 1100^{o} C by catalytic decomposition of a precursor containing carbon. The type of graphitic structures formed, closely depends on the dimensions of theses metal catalyst particles [24][25]. Growth of these structures have been shown repeatedly to be effective on iron (Fe), Nickel (Ni) and

Cobalt (Co) [26]. Andrews et al. have demonstrated the growth of MWCNTs via chemical vapor deposition and have proposed a growth model for these structures [27]. A combination of factors is responsible for the growth of these ordered carbon structures on such metal films. These factors include catalytic activity of the metal particles to decompose carbon compounds, ability to form stable metal carbides, and rapid diffusion of decomposed carbon through and into these metal particles.

In the case of growth on thin films, carbon from the precursor dissolves into the metal film and upon cooling, precipitates on the surface as a thin film of highly crystalline graphite with the basal planes parallel to the substrate. In a floating catalyst method, (which has been utilized for CNT growth in this study) metal particles are introduced along with the precursor, which fall onto the substrate thus, promoting growth of carbon filaments of similar diameter. Carbon diffuses into these metal particles along the concentration gradient and precipitate on the other half of the particle. However, precipitation doesn't take place on the top most point of the metal particle, which explains the hollow core present inside these filaments. In this structure, the graphitic basal planes are tangential to the curved surface of the metal particles [27]. Filament growth on supported metal particles can be of two types, (i) extrusion, in which the filament grows upwards from the surface of the metal particle, which remains adhered to the substrate, (ii) tip-growth, in which the filament grows from beneath the metal particle, thus detaching it from the substrate [24].

The curvature of the metal surface plays an important role on the basal planes of the filaments formed. Therefore as the metal particle size reduces (which in turn increase the curvature), strain on the basal planes of these filaments also increases thus, promoting the growth of a continuous surface that is energetically more favorable. This is how multi walled carbon nanotubes are formed. If the particle size is further reduced, single walled carbon nanotubes are formed.

The same growth mechanism theory can be used to explain the MWNT site selective growth on Au patterned quartz substrate via a floating catalyst method. During CVD, the nucleation of the floating iron catalyst particles falling on the Au film might be affected because of the localized surface energy of the film. Also, site selective decomposition of ferrocene particles on the oxide surface is possible. Huang et al. achieved a site selective growth of CNTs on silver patterned silicon oxide substrate [28]. EDX line analysis results showed fewer iron particles on the silver film when compared to the oxide surface. Gold and silver being present in the same group of the periodic table might also be the reason for this CNT growth prohibition.

2.4. Device Structure and mathematical modeling

In view of the potential applications of carbon nanotubes in gas sensing and the ability to achieve site selective growth of carbon nanotubes on Au patterned oxide substrates, the following device structure was conceived as shown in Figure 2.4

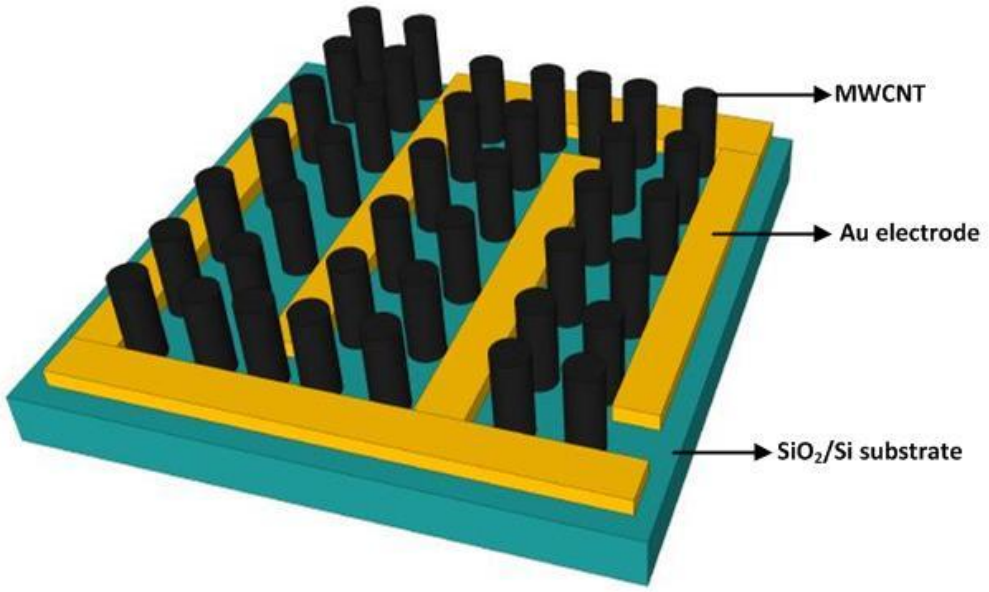

Figure 2.4: Sensor device structure showing the nanotubes between the interdigitated electrodes made of gold

This device structure consists of an in-situ grown oxide layer on a silicon substrate. Interdigitated electrodes made of Au are patterned on the oxide upon which MWNTs are grown.

To understand the operation of any device, it is necessary to study its mathematical model which is crucial for predicting its performance and its response under given conditions. Therefore, it is of utmost importance to derive a mathematical model for any newly built electronic device. An abstract model is derived for the sensor shown in Figure 2.5 and is presented here.

Figure 2.5 shows the top and cross sectional view of the interdigitated electrode configuration of the sensor. The schematic gives an idea of the variables of the electrodes. The variables associated with this model are as given below

L - Length of the electrode finger in meters

d - Distance between two fingers in meters

w – Width of each finger in meters

h – Height of each finger in meters

N – Number of fingers (5 in this case)

ε_r - Dielectric constant of the medium present between each finger (CNTs+air)

σ - Conductivity of the medium present between each finger

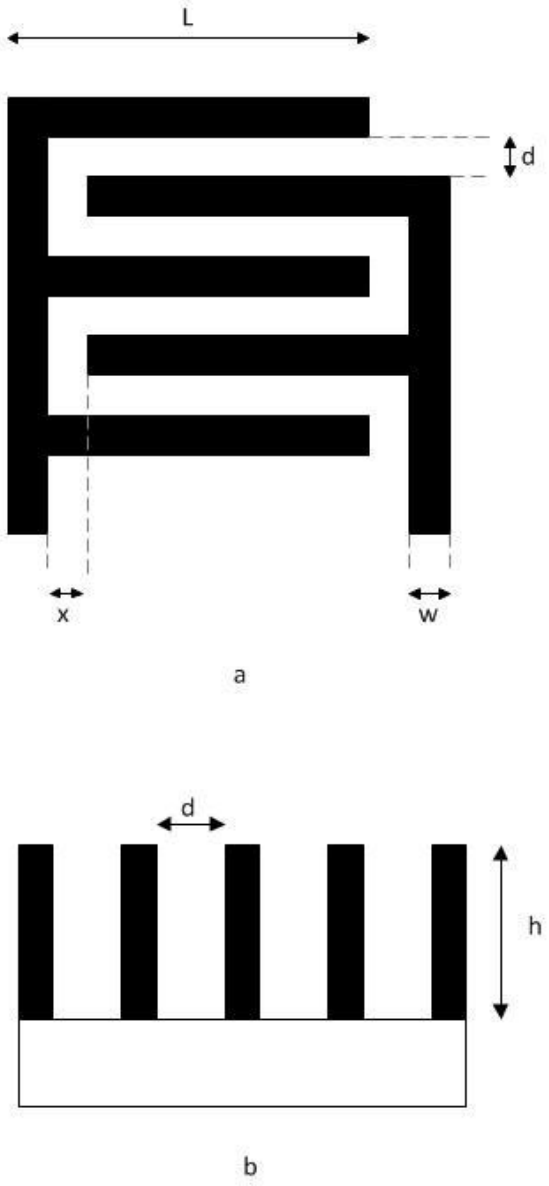

Figure 2.5: Schematic of the interdigitated electrodes. (a) Top View. (b) Side View

The sensor can be modeled as a capacitor with capacitance C in parallel with a conductance G as shown in Figure 2.6

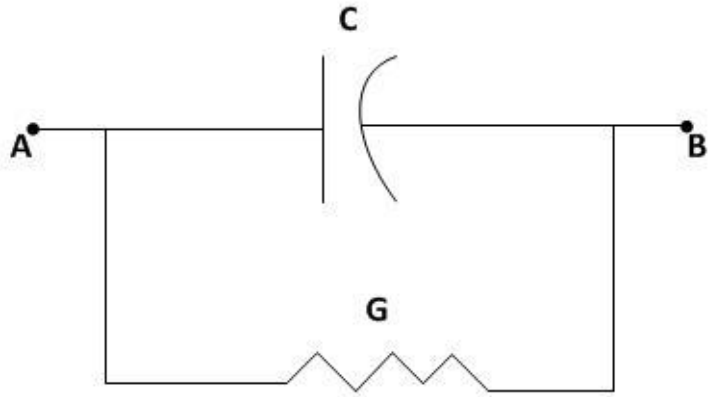

Figure 2.6: Equivalent circuit for the sensor

The total capacitance of the device can be calculated from the capacitance of a single unit cell from the expression below

$$C_{Total} = \{C_{L-X} + C_d\}(N-1) \quad (1)$$

where C_{L-X} is capacitance contributed by the dielectric present between the horizontal fingers. C_d is the capacitance contributed by dielectric between the vertical fingers. Since these two capacitances are in parallel, their contribution adds up to the total capacitance.

Similarly the total conductance of the device is given by the expression

$$G_{Total} = \{G_{L-X} + G_d\}(N-1) \quad (2)$$

The C_{L-X}, C_d , G_{L-X} , $G_d$components of a unit cell are shown in Figure 2.7.

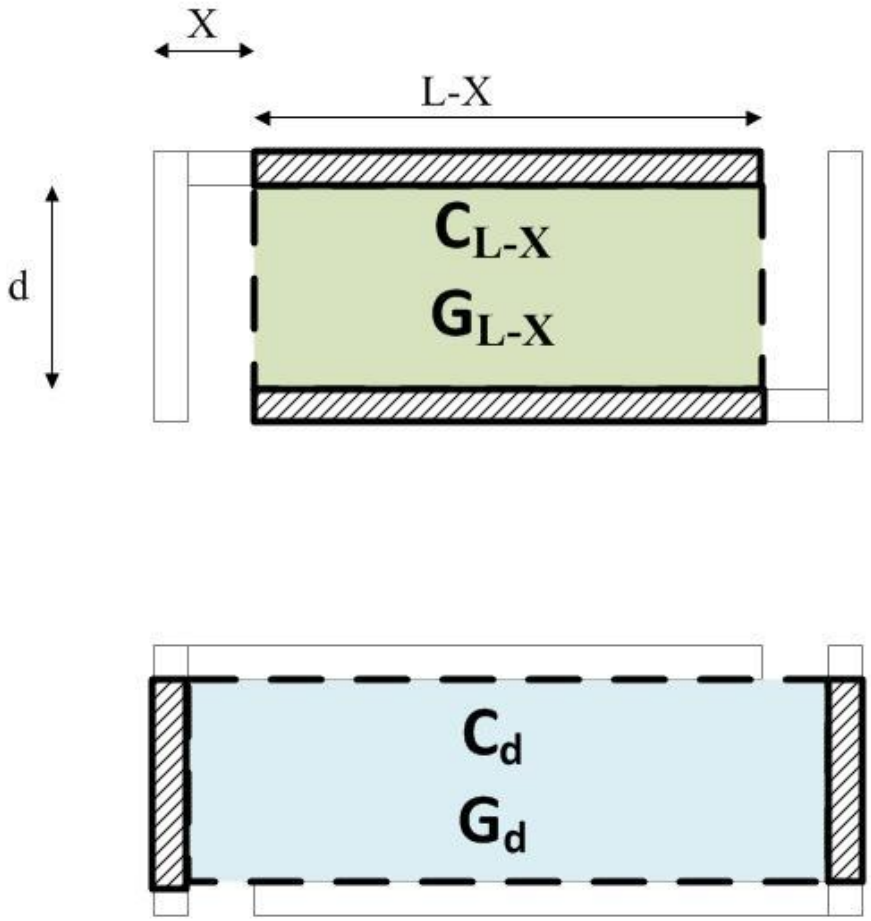

Figure 2.7: Capacitance contributions C_{L-X} and C_d to the unit cell.

The total capacitance of the device in room conditions without CNTs (which is a known value from experimental measurement) is contributed by electrical field through the air

between the plates and through a small layer of silicon oxide beneath the elctrodes. The electriclal field configuration for such a device is shown in Figure 2.8

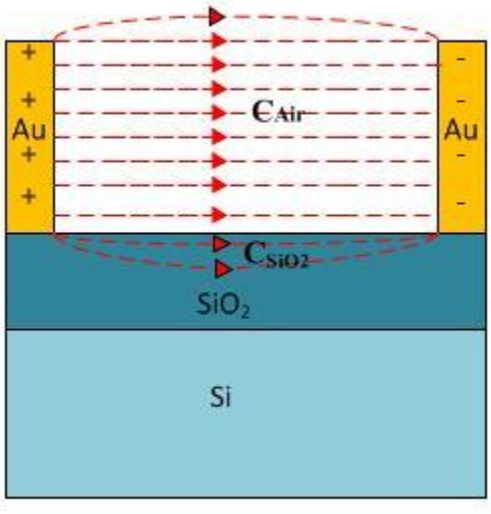

Figure 2.8: Electrical field lines through air and the oxide layer beneath the electrodes

The total capacitance of the device in air without CNTs is given by the expression

$$C_{Total}{}^{air} = C_{air} + C_{SiO2} \quad (3)$$

where C_{air} is the component contributed by air and C_{SiO2} is component contributed by the oxide.

After the growth of MWCNTs, the electrical field configuration of a unit cell can be considered as in Figure 2.9. Field lines through oxide are neglected for an easier model.

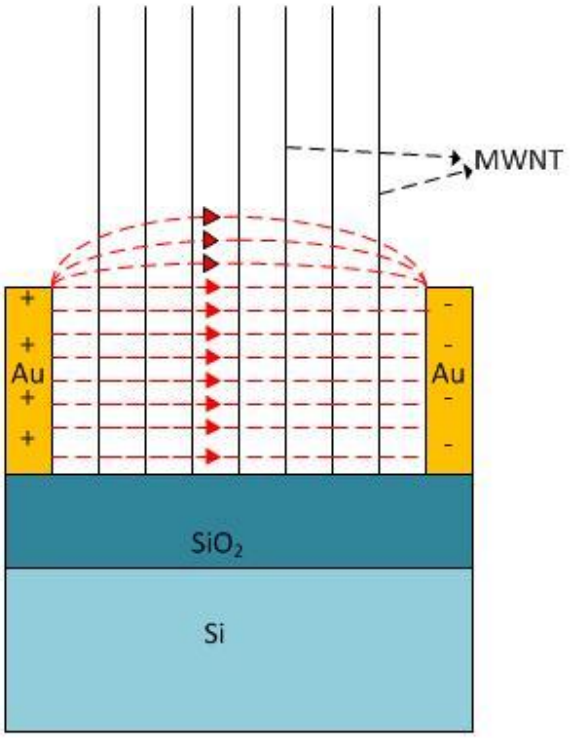

Figure 2.9: Electrical field lines through air, CNTs between the electrodes and through the underlying oxide

For calculation of *L-X* and *d* component,

$$C_{L-X} = \varepsilon_r * \frac{(L-X)h}{d} \quad (4)$$

It is to be noted that ε_r is a function of frequency and can be calculated only for a frequency at which measurements were done. Also, ε_r is dielectric constant of the whole medium (CNTs+gas) present between the electrodes. Similarly the other component is given by

$$C_d = \varepsilon_r * \frac{dh}{L+X} \quad (5)$$

Therefore the total capacitance of the device can be calculated from equations (1),(4) and (5).

From Fig 2.6 the conductance contributed by the *L-X* and *d* component is given by

$$G_{L-X} = \sigma * \frac{(L-X)h}{d} \quad (6)$$

$$G_d = \sigma * \frac{dh}{L+X} \quad (7)$$

The total conductance can be calculated from equations (*2*), (*6*) and (*7*).

3. Experimental procedures

3.1. Fabrication

Fabrication of a gas sensor, using the CNT growth confinement technique mentioned in section 2.3, requires utmost care and diligent handling of the device throughout the fabrication process. Figure 3.1 illustrates the flow of the fabrication process.

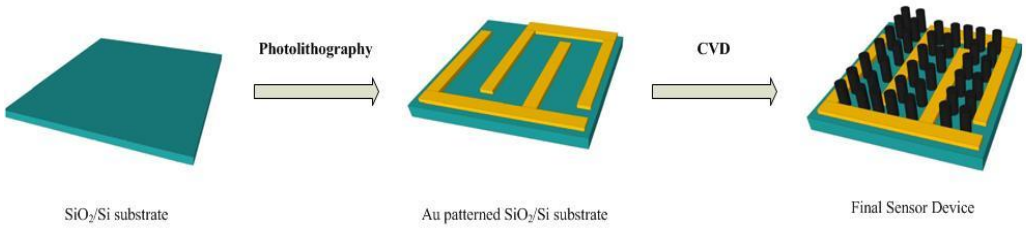

Figure 3.1: Outline of fabrication process for the gas sensor

The entire process of fabrication can be classified into three categories: (i) SiO2 growth by thermal oxidation (ii) Photolithography and Lift off procedures for patterning of gold interdigitated electrodes. (iii) MWNTs growth via chemical vapor deposition

(i) SiO2 growth by thermal oxidation:

To obtain a passive insulating layer on a p-silicon substrate a thin layer of oxide is grown using the thermal oxidation. This layer of oxide is essential for the isolation of the MWNTs from the semiconducting silicon throughout the fabrication and measurement process. Standard RCA cleaning procedures were employed for the thorough cleaning of the p- silicon wafers. Wafers were immersed in a 5:1:1 H_2O:H_2O_2:NH_4OH solution at 80^o C for 10 minutes to get rid of any organic impurities present on the silicon surface, followed by a thorough rinse in DI water. During this step, a thin layer of silicon oxide is formed due to the metallic impurities present on the surface. A short immersion in a 50:1 H_2O:HF solution at room temperature removes this oxide layer and other metallic contaminants. Wafers undergo a thorough DI water rinse before the last step, which involves immersion in a 6:1:1 H_2O:H_2O_2:HCL solution at 80^o C .This step effectively removes any remaining traces of metallic impurities left on the silicon surface. [29].

Cleaned wafers were loaded into a Lindberg High Temperature furnace at an ambient temperature of 800^o C. The furnace undergoes a nitrogen flush for 30 minutes to remove any contamination inside the tube furnace. The temperature was hiked to 1100^o C after wafer loading. Oxygen gas was pumped into the tube for 30 minutes at a flow rate of 500sccm after the temperature reaches 1100^o C. This is followed by post oxidation

annealing in nitrogen with the gas flowing at 1000 sccm for 2 hours. Finally the furnace was switched off and the wafers were allowed to cool down before taking them out.

(ii) Patterning of Au interdigitated electrodes on SiO_2 /Si substrate:

Oxidized silicon wafers cut into smaller substrates of about 1 inch by 1inch undergo a thorough rinse with acetone, Isopropyl alcohol (IPA) followed by DI water. S1813 positive photo resist spun on each substrate at 4000 rpm formed the photo sensitive layer on the substrate. The substrates were soft baked at 95^{o} C for 1 minute. Ultra violet exposure (350nm~500nm) of about 12 seconds formed the patterns on the photoresist defined by the photomask using a Karl Suss MJB-3 mask aligner. The substrates went through a development process in MF-319 solution for about 30 seconds at room temperature, followed by a DI water rinse. The substrates were hard baked at 115^{o} C for about 3 minutes to harden the remaining photoresist.

After defining the patterns on the substrate, gold was sputtered on to these substrates using argon plasma inside a sealed chamber maintained approximately at 3~4 milli torr. Prior to gold deposition, a titanium layer of about 5 nm was sputtered, which served as a seed layer for gold film .The seed layer ensures better adhesion of gold film on the substrate and plays an important role during lift off process. Power of the RF gun was maintained at 35 watts and the purity of the gold target was 99%. A Controlled deposition rate of 7 A^{o}/min was utilized to get a film of 1 micron thick. To obtain the final pattern of gold, the substrates were immersed in S1165 solution at 80^{o} C for about 5 minutes followed by a short ultra-sonication in IPA. This process removes the hardened photoresist defined by the patterns along with the gold film present on the resist.

(iii) MWNTs growth via chemical vapor deposition

Multi walled carbon nanotubes were grown on the sample by a process described by Andrews et al. [30]. Patterned samples were loaded into a Lyndberg tube furnace with a diameter of 96 mm. The furnace was heated to 750^{o} C in an argon atmosphere with the flow rate controlled at 750 sccm. The tube was purged with hydrogen gas at a flow rate of 75sccm after the temperature reached 750^{o} C. Ratio of 9:1 for Ar/H_2 inside the CVD chamber was ensured. A ferrocene and xylene mixture in a ratio of 1:0.1148 (11.48 gms of ferrocene per 100gms of xylene) was pumped into the CVD chamber at a rate of 30 ml/hr for about 2 minutes until the vapors are visible at the other end of the tube. This rate was then reduced to 3ml/hr for the whole synthesis. After a synthesis time of 10 minutes, the hydrogen flow was cut off immediately and the syringe pump was stopped and withdrawn. Samples were allowed to cool down in argon and then removed.

3.2. Measurement

After the CVD growth, the MWCNT based gas sensor is ready for evaluation for its capacitance and conductance response to an analyte gas exposure. The sensor was kept in a sealed chamber equipped with gas inlets and probe connections for measurement. IDE electrodes were connected to the probes which were in turn connected to an HP 4192A impedance analyzer. Prior to measurement, the setup underwent an open and closed compensation to remove any errors, contributed by the parasitic capacitance offered by the probes and the test fixture. Capacitance and conductance response was monitored continuously and recorded every minute for a frequency range of 20 kHz to 1000 kHz,

with a step size of 20 khz. Before the sensor evaluation, N_2 was flushed into the test chamber for about 30 minutes. Alternate cycles of N_2 and analyte gas were flushed into the chamber, such that each cycle lasted 10 minutes long. Flow rates of N_2 and analyte gas were 1000sccm and 500sccm respectively. The experimental setup is shown in Figure 3.2 below.

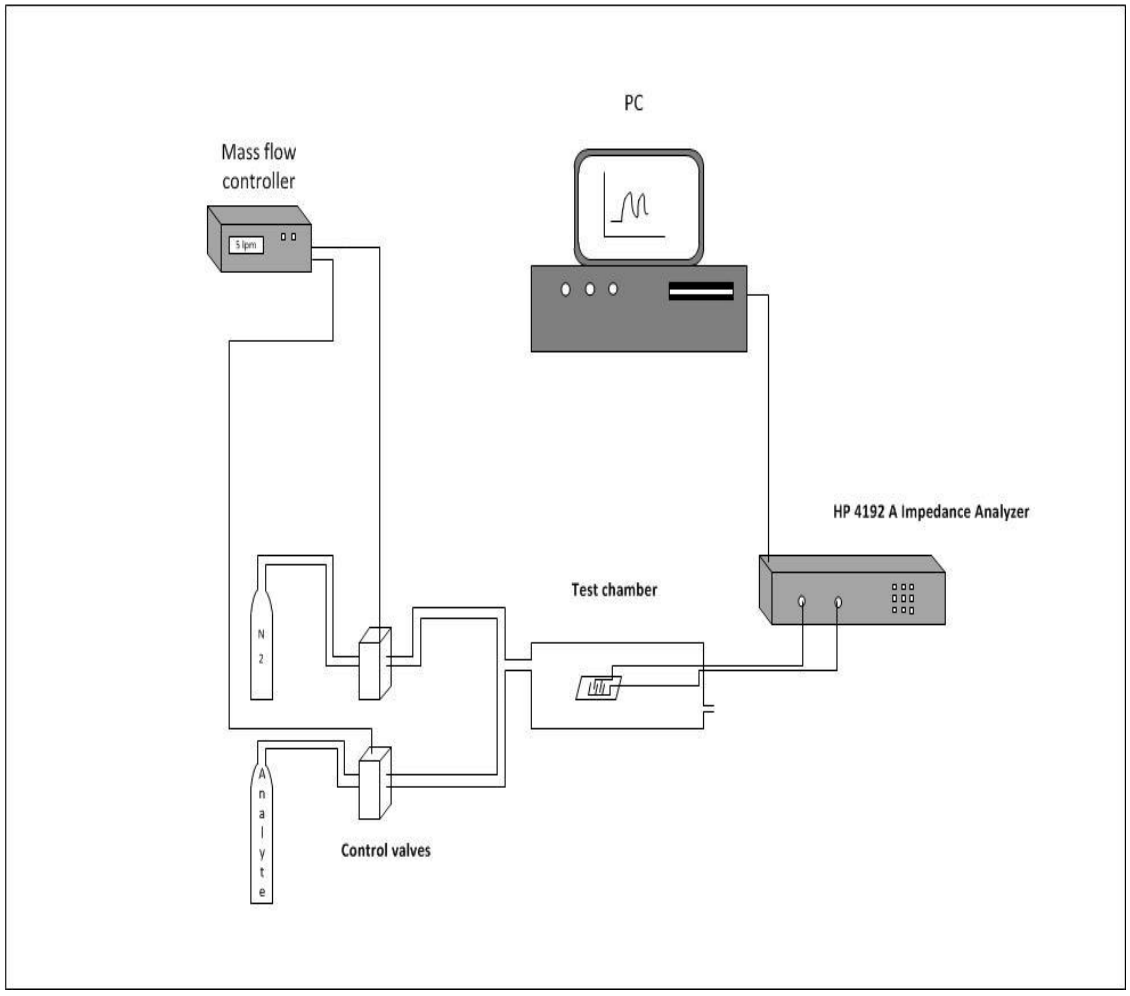

Figure 3.2: Experimental setup for the capacitance and conductance response measurement of a sensor

4. Results and Discussions

4.1. Scanning Electron Microscopy Observations:

As discussed in the previous sections, only site-selective growth of MWCNT's on Au/SiO_2 surfaces via floating catalyst methods have been reported. This is the first time that a device has been fabricated, using this growth confinement technique for MWCNT's on Au/SiO_2 surfaces. Figure 4.1 shows a photograph of a sensor built using this principle. It can be observed that MWCNTs grew selectively on the oxide surface between the electrodes.

Figure 4.1: Sensor with the MWCNT's grown in between the gold inter-digitated electrodes.

Figure 4.2 shows the SEM images of the sensor from various views. The top view of the sensor is shown in Figure 4.2a which gives an indication of the difference in growth morphologies on the gold electrodes and the SiO_2 surfaces in between. Figure 4.2b gives the side view of the device that illustrates the MWCNT's growth pattern on the electrodes and the oxide layer. The micrographs clearly indicate minimal growth of MWCNT's on the electrodes as conceived in the previous section. This can be attributed to the negative effect of the gold film on the nanotube growth as demonstrated by Cao et al. [21]. The ferrocene catalyst particles on the oxide surface are able to promote a dense growth of MWCNT's whereas the catalytic activity of the same ferrocene particles on the gold surface seems to be severely inhibited. Vajtai et al. reported the cause of this site selective growth to be due to the presence of pure gamma iron (FCC Fe) particles on the silicon oxide surface which is an excellent catalyst for MWCNT growth [31]. The cause of this site selective growth could be due to the difference in binding energies of iron particles on the oxide and gold films. Localized surface energies of the gold film, prohibiting the nucleation of the iron particles is also a possibility.

Figure 4.3(a) shows a magnified view of the MWCNT's on the silicon oxide surface. The micrograph illustrates an aligned growth of MWCNT's, length of about 50 microns similar to the conventional CVD growth achieved by Andrews et al. [30]. Figure 4.3(b) shows the top view of the nanotubes present on the oxide layer. The MWCNT's seem to get entangled at the top after a particular length of aligned CNTs has been obtained. A highly magnified view of the nanotubes along with some particles adhered to them is displayed in Figure 4.4 a. This concurs with the results obtained by Cao et al.[21] to a similar CVD growth process on gold patterned quartz substrates. These are suspected to

be gold particles chipped off from the electrode film that get stuck to the nanotube surface during the CVD process. Figure 4.4(b) shows an image of the nanostructures sprouted from the sparsely distributed fissures on the gold film. Growth of nanotubes on the oxide surface, beneath the gold film could be the reason for these fissures. Breakdown of the gold film can also be a result of a complex thermal dynamics during the CVD process.

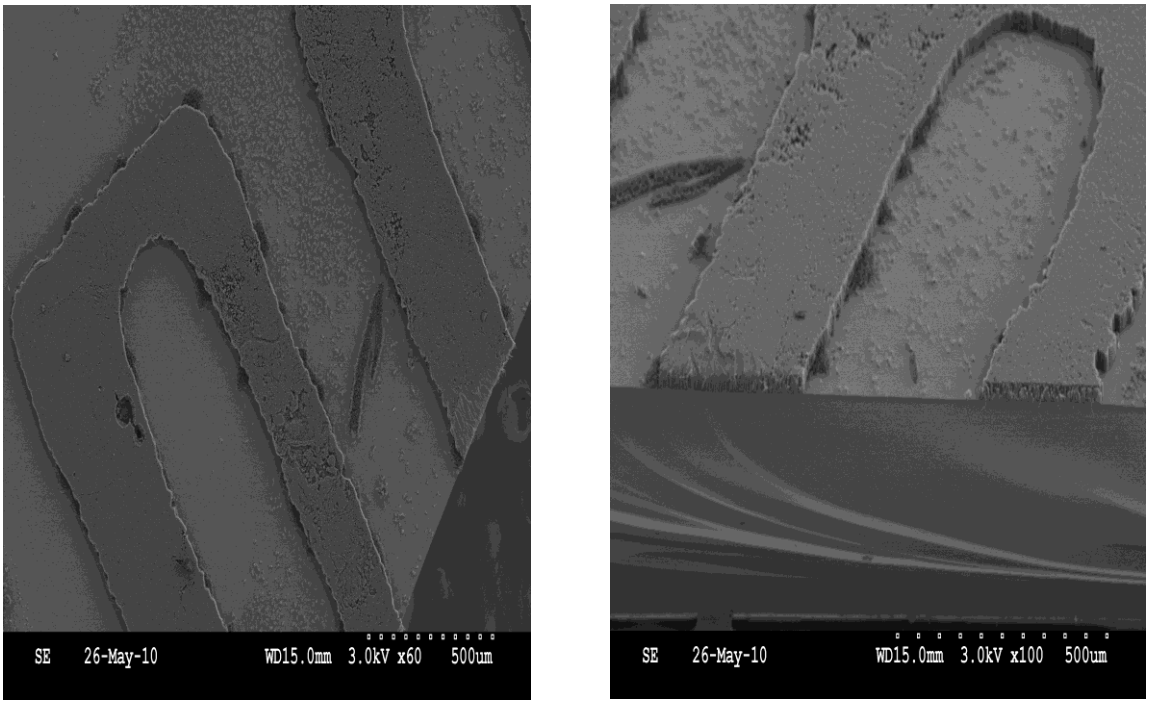

(a) (b)

Figure 4.2: (a) SEM image with a magnified view of the top view of the sensor. (b) Cross sectional view of the sensor

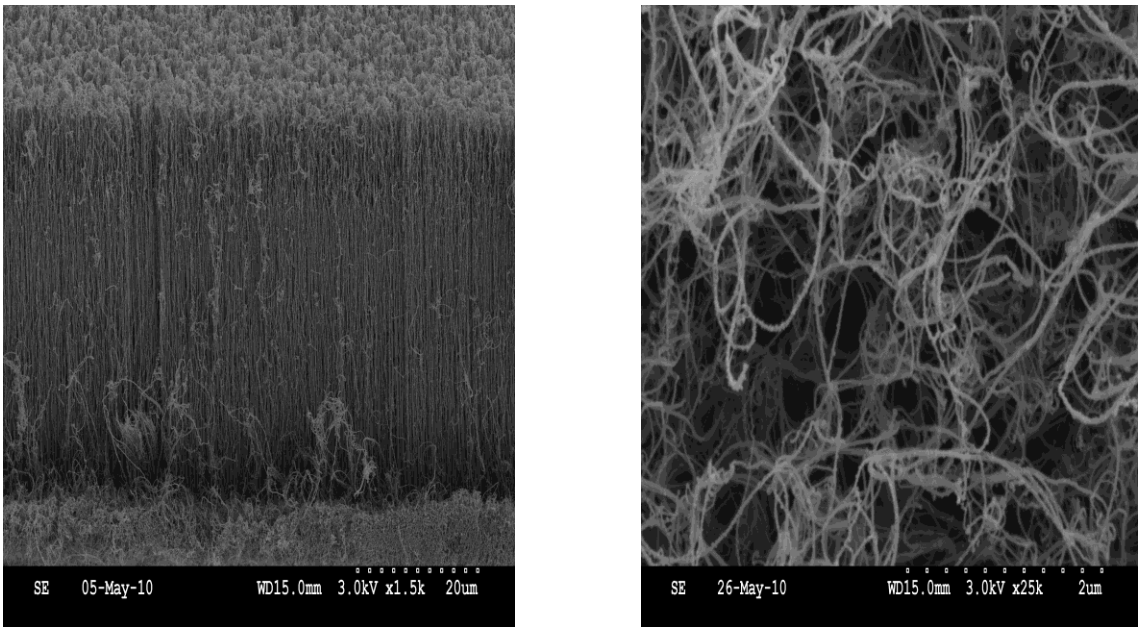

(a) (b)

Figure 4.3: (a) Aligned growth of MWCNT's on the oxide surface. (b)Top view of the MWCNT's

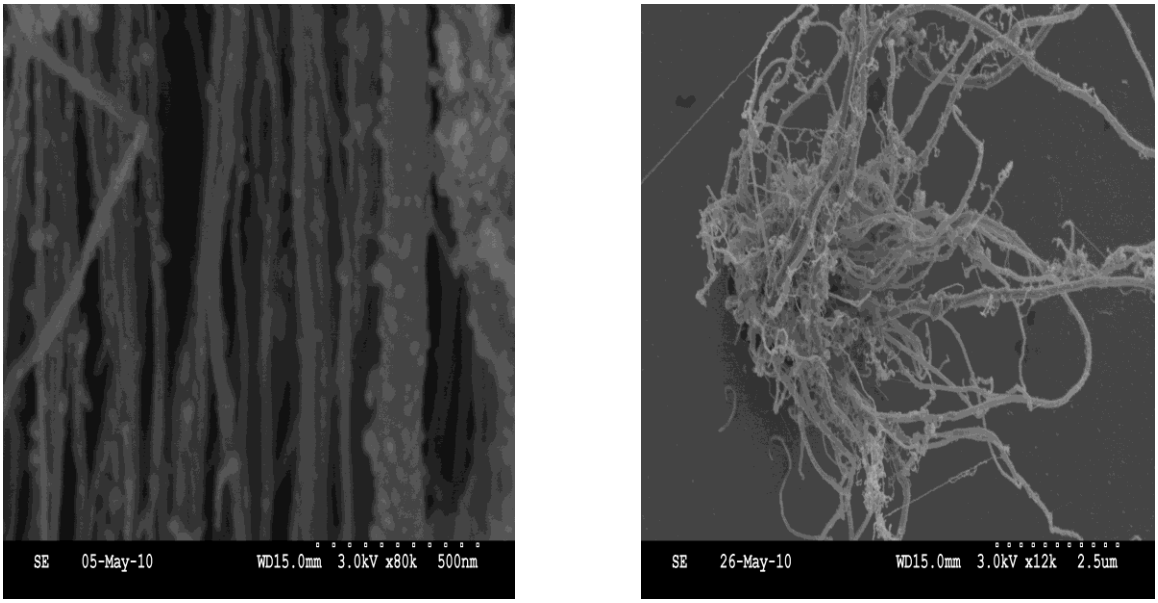

(a) (b)

Figure 4.4: (a) Highly magnified image of the nanotubes. (b) MWCNT's growth from the fissures on the gold film.

From the SEM images it can be concluded that a good control of site selective growth has been achieved and a sensor device has been fabricated, to a large extent that is similar to the proposed device structure. However it would be interesting to see the performance of this device for a test gas in real time environment.

4.2. Sensor Results:

Figure 4.5 below shows the $\frac{G}{\omega C}$ value versus frequency for the device. The plot shows that the device obtained is a conductive device. However it would be interesting to see the capacitance response for this device to a gas exposure, along with its conductance response.

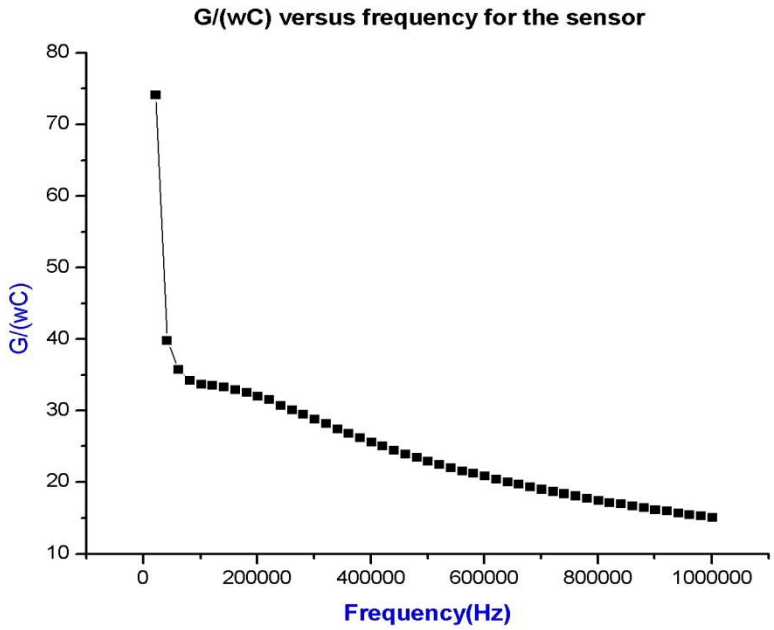

Figure 4.5: $\frac{G}{\omega C}$ variation with frequency plot

4.2.1. Capacitance Response:

The capacitance versus frequency plot of a sensor is shown in Figure 4.6. It illustrates the effect of CNT's as a dielectric, on the capacitance of the device against the frequency. After the nanotube growth, the capacitance of the device increased almost by a factor of 20 for lower frequencies of measurement. As the frequency increases this factor decreases, but the value is still larger when compared to the device without the CNT's amidst the electrodes. As the change in the dimensions of the electrodes is minimal before and after the CVD, the increase in capacitance could be the result of an increase in conductivity of the device which has a secondary effect on the capacitance of the device.

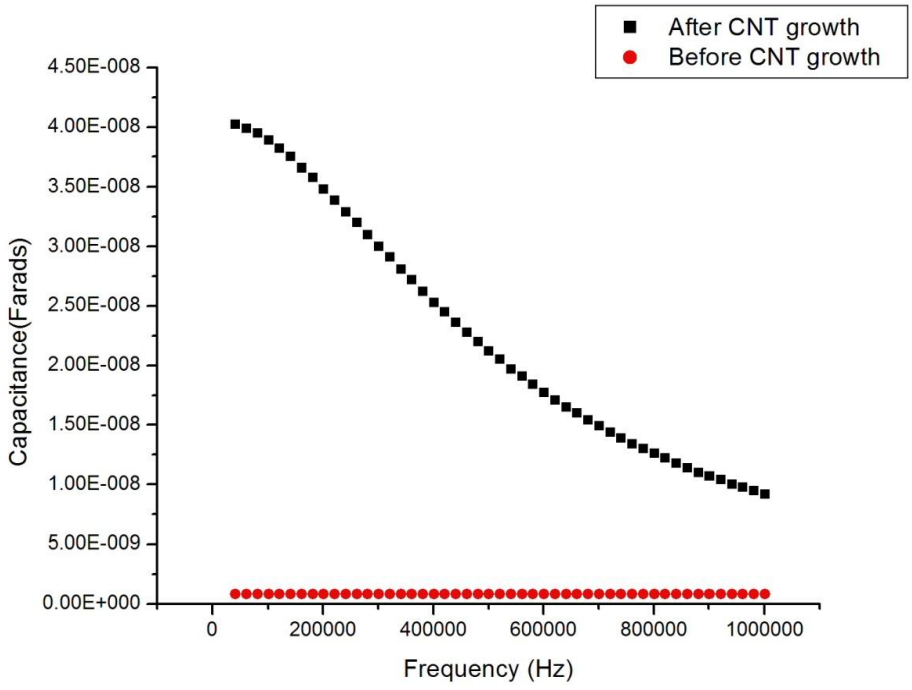

Figure 4.6: Capacitance against frequency plot for a sensor before and after the growth of MWCNTS.

The performance of a sensor for 0.01% NO_2 gas can be seen in Figure 4.7. The plot shows the capacitance response of the device at 201 kHz to alternate cycles of N_2/NO_2 gases exposure, each cycle lasting 10 minutes each. When exposed to NO_2 gas, capacitance of the device decreases, which can be attributed to the adsorption of gas molecules on the inner walls of the nanotubes which in turn has an increasing effect on the overall conductivity (which has a secondary effect on the capacitance). A small effect on the dielectric constant is also a possibility. During N_2 purge, the capacitance of the sensor increases as the weakly bonded physisorbed gas molecules desorb, decreasing the net conductivity of the device.

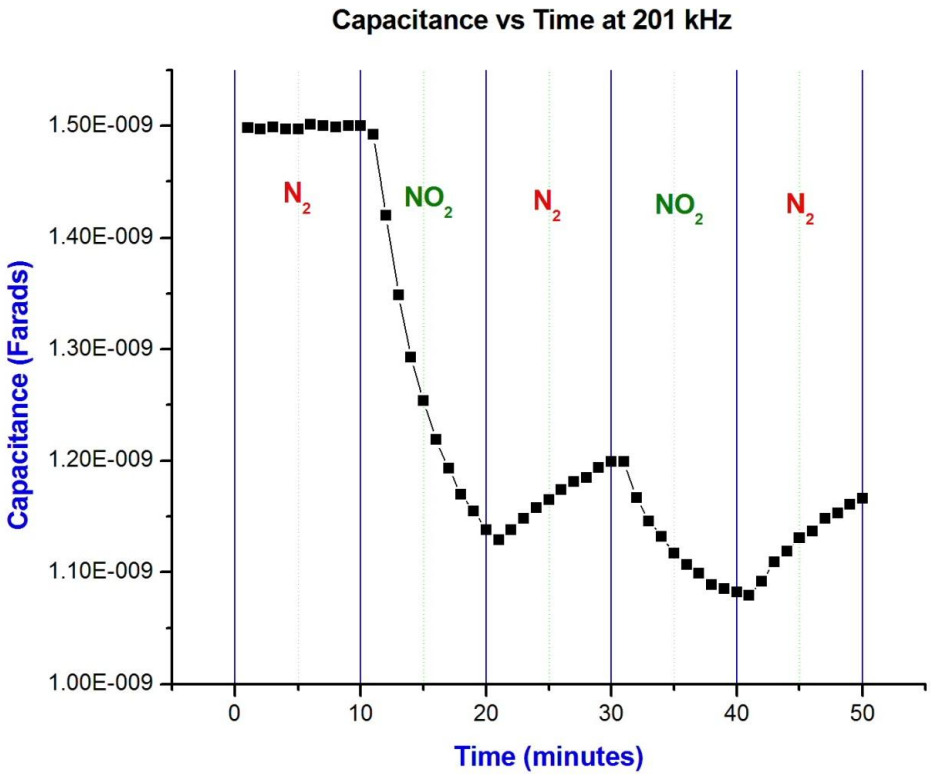

Figure 4.7: Capacitance against time response of the sensor for alternate cycles of N_2/NO_2, each cycle lasting for 10 minutes each. Concentration of NO_2 being 0.01%.

The device response was recorded at four different frequencies 21kHz, 201kHz, 401kHz and 801kHz simultaneously. The sensor doesn't seem to respond to the test gas at lower frequencies, however for higher frequencies above or in the range of 201 kHz the device gives a response to the test gas. Response at 401 kHz and 801 kHz is shown below in Figure 4.8

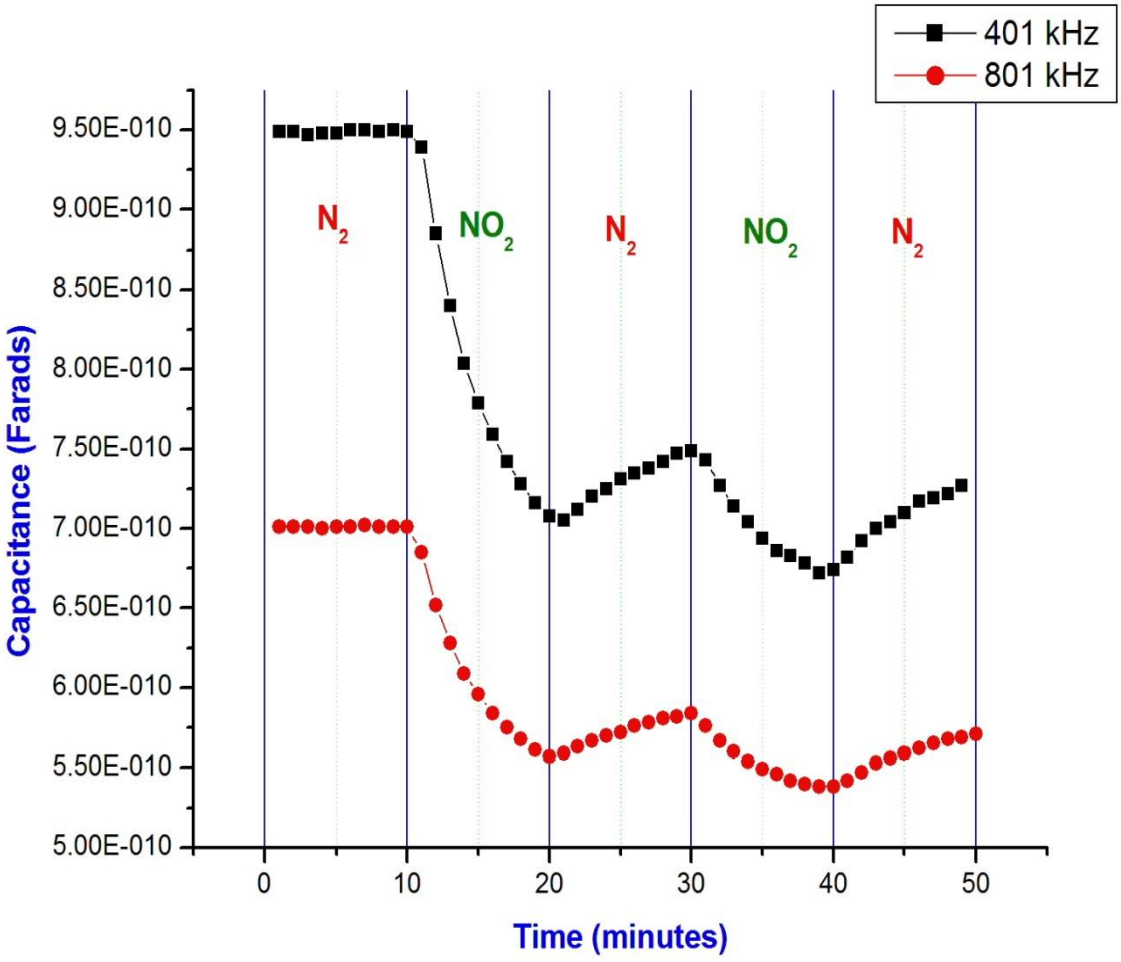

Figure 4.8: Capacitance response for alternate cycles of N_2/NO_2 gases at 401 kHz and 801 kHz.

The capacitance against time response plots in Figures 4.6 and 4.7 gives a fair idea, as to how the test gas NO_2 has an effect on the sensor. However percentage sensitivity, a parameter of the sensor is also critical for qualitative analysis of the sensor. % Sensitivity of the sensor used for test gases is calculated as given below

$$\%\, Sensitivity = \frac{C_{gas} - C_{N2}}{C_{N2}} \quad X \quad 100 \qquad (8)$$

Where C_{gas} is the capacitance of the sensor when exposed to the test gas and C_{N2} is the value during N_2 purge. Percentage sensitivity was thus calculated for every minute of the test run using the above expression and is plotted against time. Such a plot is shown in Fig 4.9 where it illustrates the sensitivity profile of the same sensor at 201 kHz. The plot shows a negative sensitivity which is the result of decrease in capacitance under NO_2 exposure. A sensor response of 24.03 % for the first pulse and a cumulative response of 27.97 % is obtained for 0.01% of NO_2

Plots in Fig 4.6 and 4.8 also give an idea about the sensor recovery profile. There seems to be substantial recovery during the N_2 gas cycle. However the recovery seems to be slow and not complete. This is due to poor desorption of the strongly bonded gas molecules at the defect sites present on the surface or the inner walls of nanotubes.

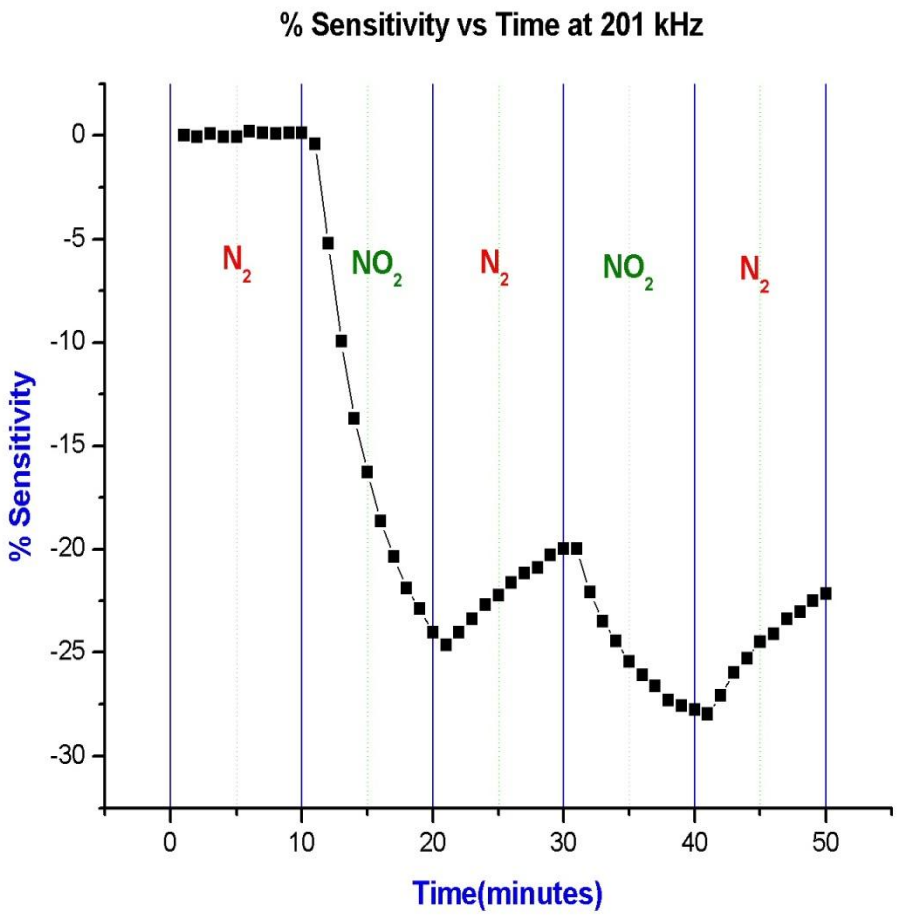

Figure 4.9: % Sensitivity versus Time plot for the sensor to alternate cycles of N_2 and 0.01% NO_2.

% Sensitivity of the above sensor for different frequencies is also plotted and shown in Figure 4.10. The sensitivity against time profile looks almost similar at all the three frequencies. However there is slight increase in sensitivity as frequency increases to 401 kHz and again decreases as the frequency increases to 801 kHz.

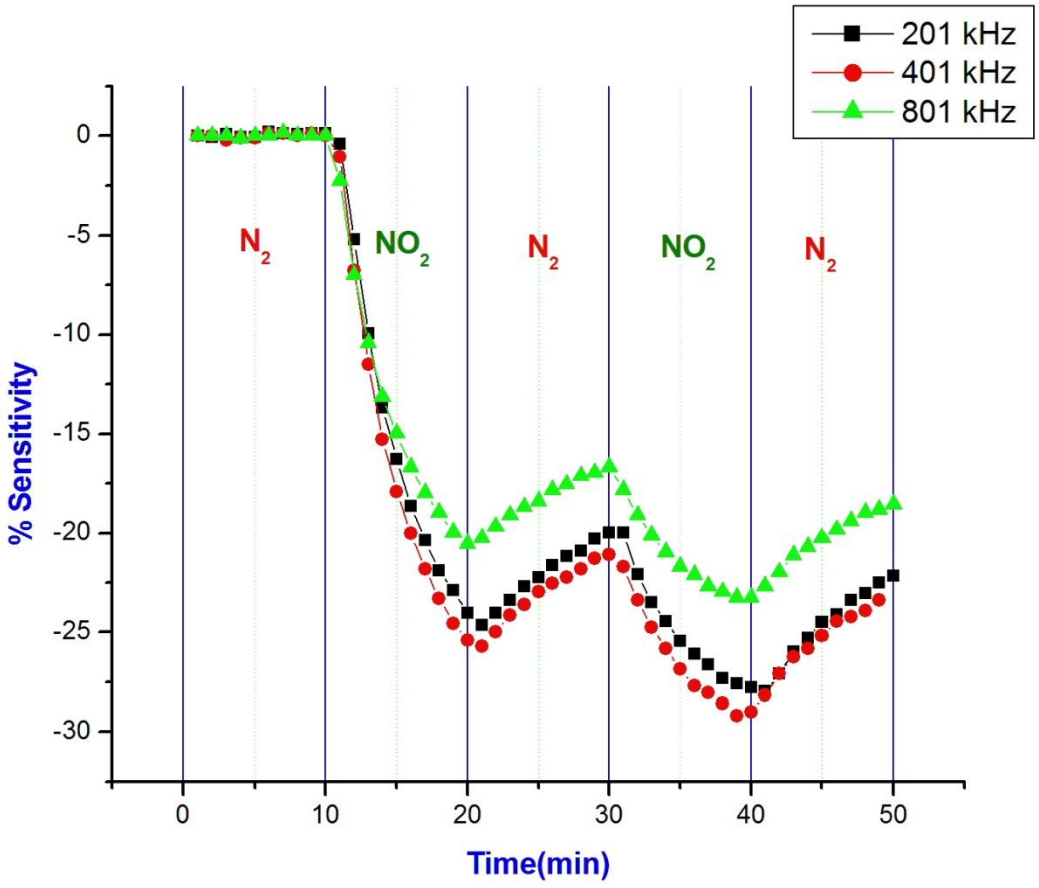

Figure 4.10: % Sensitivity versus Time plot for the sensor at different frequencies 201 kHz, 401 kHz and 801 kHz.

A study of effect of flow rate on sensitivity is done and shown in Figure 4.11. Flow rates of 100 sccm, 300 sccm and 500 sccm of the test gas have been utilized for this study. Sensitivities at 801 kHz are plotted against time for these flow rates. The plot shows that an increase in flow rate from 100 sccm to 500 sccm increases the overall sensitivity of the sensor. % sensitivity for the first pulse obtained are 4.01, 2.95 and 3.01 for the corresponding flow rates of 500 sccm, 300 sccm and 100 sccm respectively. Higher availability of gas molecules for adsorption may be the reason for this increased response.

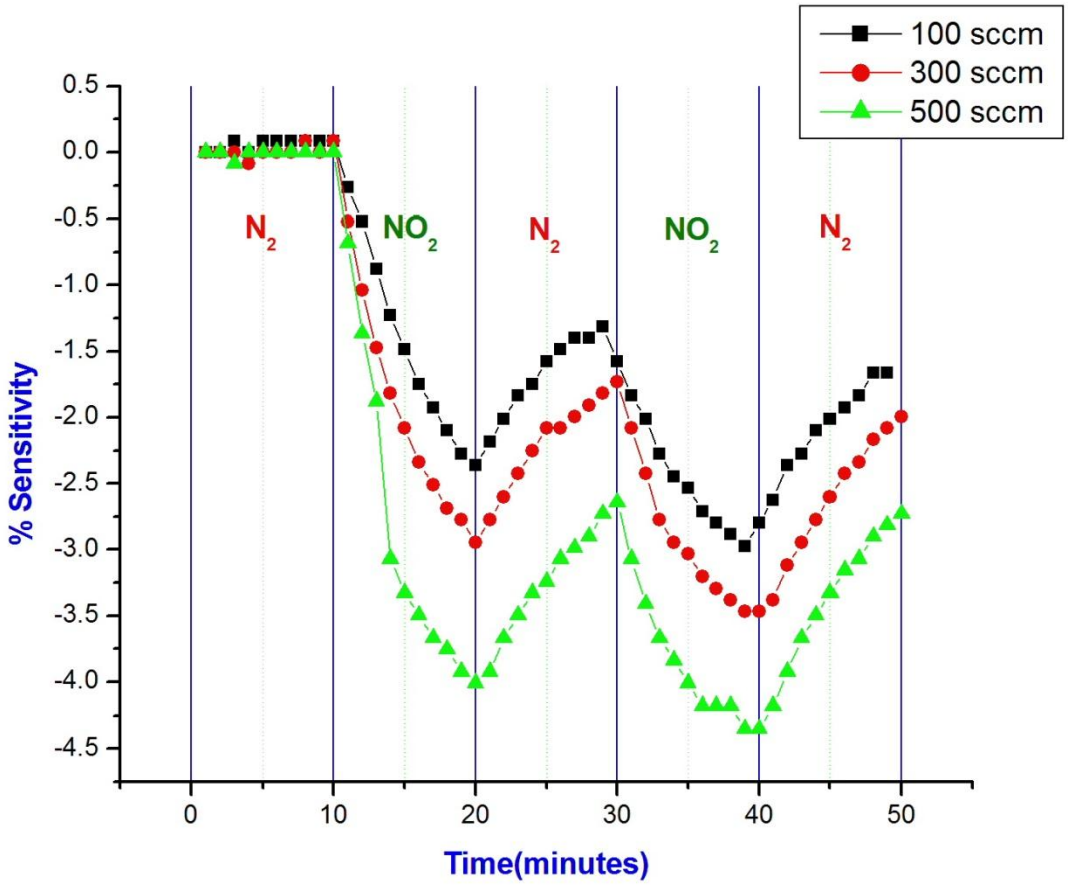

Figure 4.11: Effect of flow rate on % sensitivity for 0.01 % NO_2 test gas at 801 kHz.

4.2.2. Conductance Response

Figure 4.12 below shows the conductance response of the sensor to similar cycles of N_2/NO_2 gases at 201 kHz. It clearly shows that the conductance increases for NO_2 gas exposure which is expected of a conductance based CNT sensor. Since NO_2 is a charge acceptor it withdraws the electrons from the carbon nanotubes therefore increasing its conductivity (Since the nanotubes grown using the process mentioned in section 3, results in a p-type CNT) [32].

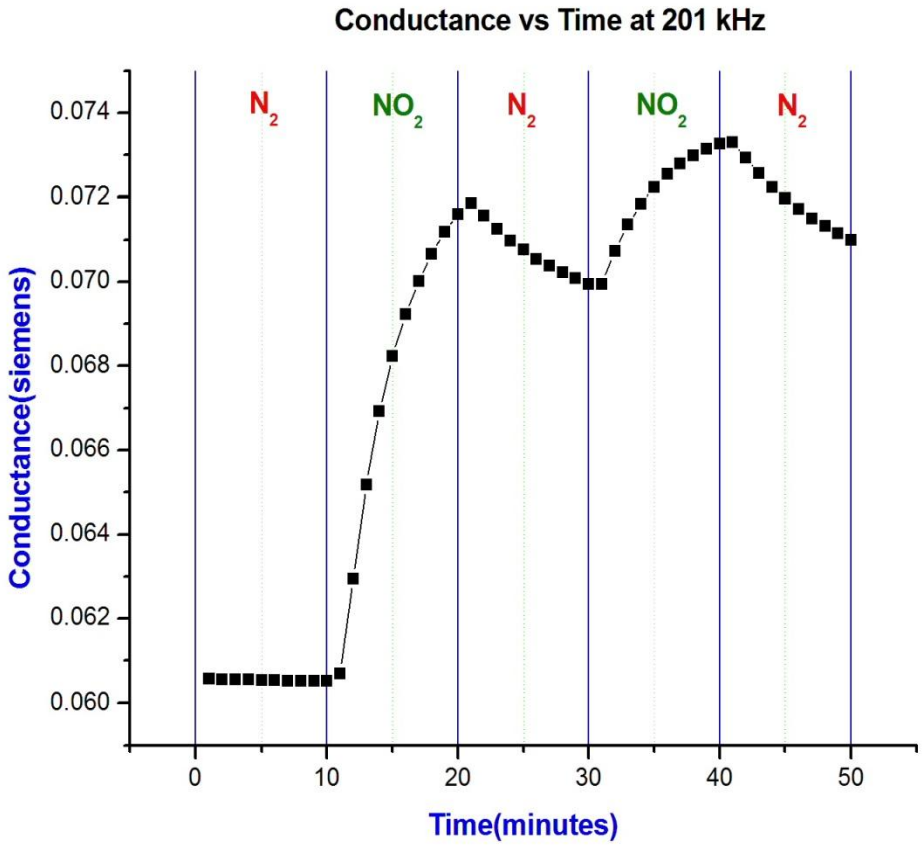

Figure 4.12: Conductance response of the sensor at 201 kHz

Also Figure 4.13: shows the conductance response at 201 kHz, 401 kHz and 801 kHz on a single plot. It can be clearly seen that all the three responses almost superimpose on each other. This is because of the frequency independent value of the conductance of the device. Sensitivity for conductance response is calculated in a similar fashion as given by equation

$$\%\, Sensitivity = \frac{G_{gas} - G_{N_2}}{G_{N_2}} * 100 \qquad (9)$$

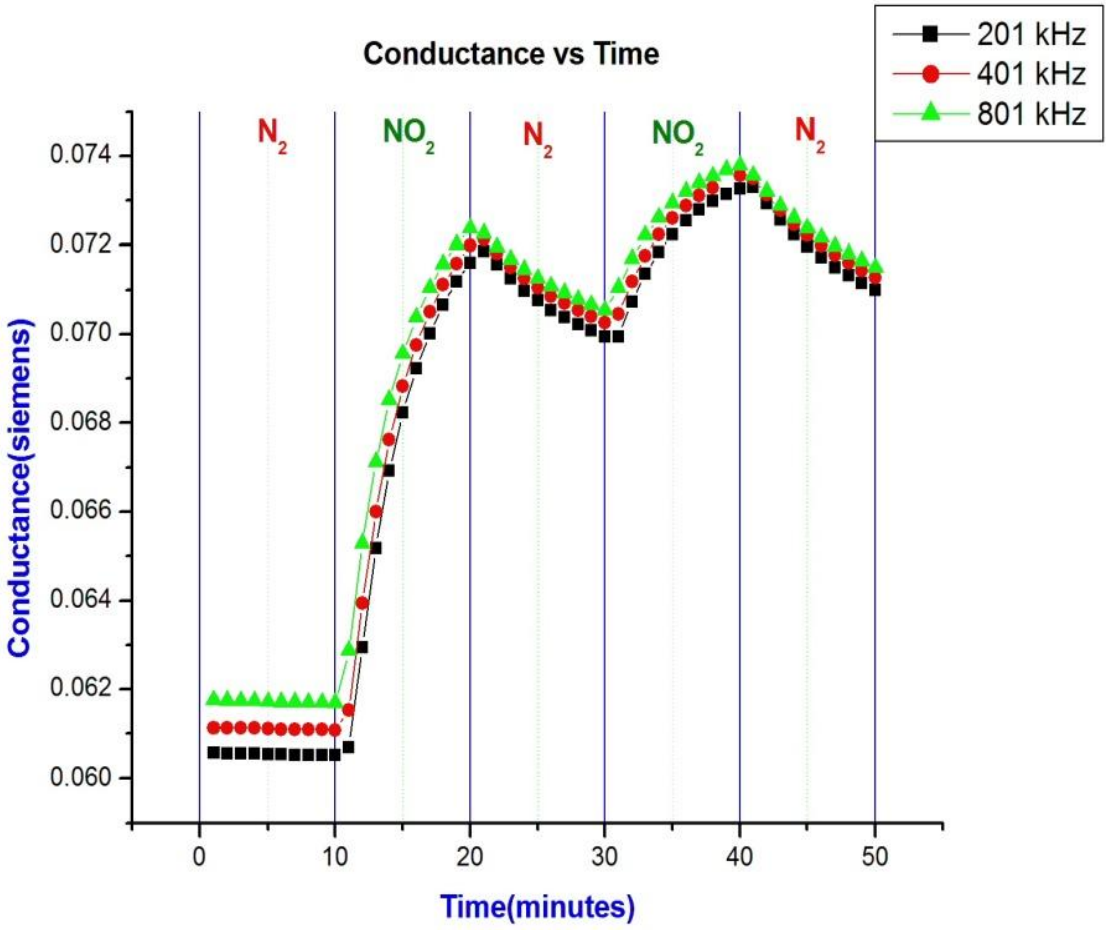

Figure 4.13: Conductance against Time at different frequencies

Figure 4.14 shows the percentage sensitivity against time profile for the conductance response of the sensor at different frequencies. A percentage sensitivity of 18.63 for the first pulse and an overall sensitivity of 20.01% have been achieved at 201 kHz.

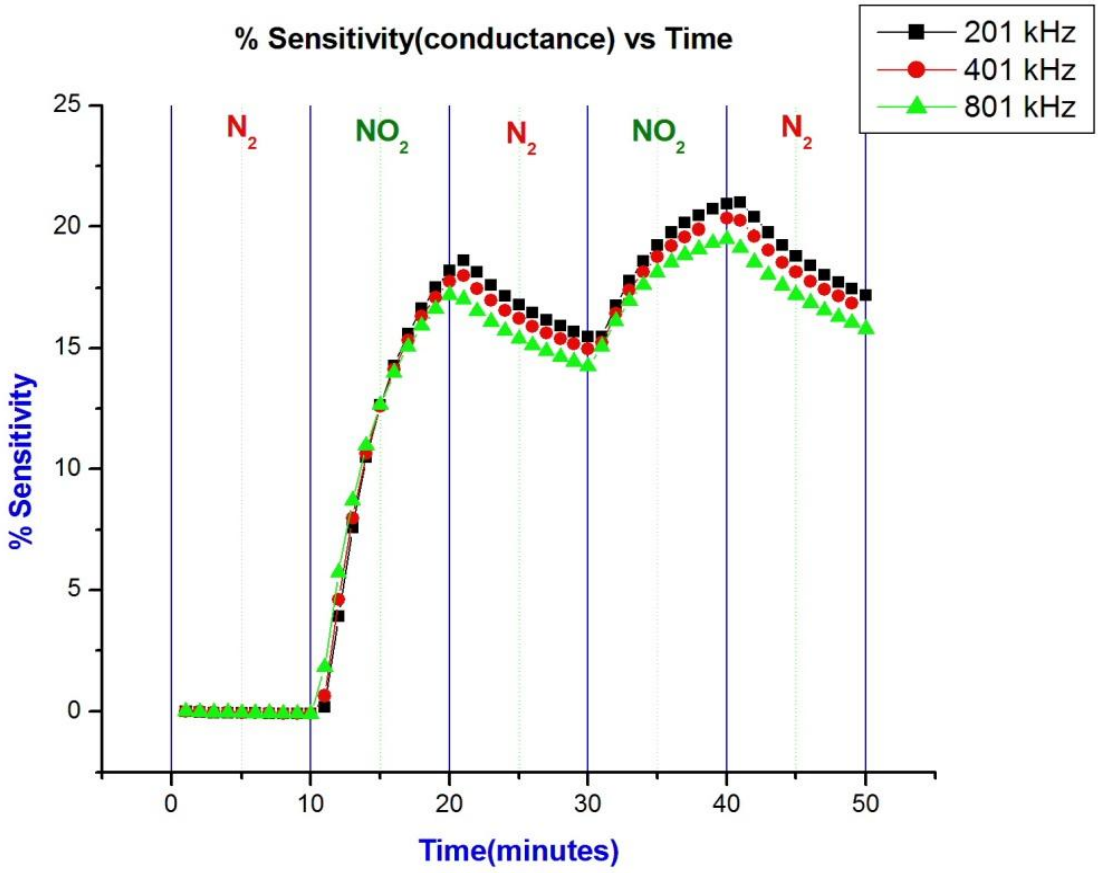

Figure 4.14: Plot for %sensitivity (conductance) against time at 201 kHz, 401 kHz and 801 kHz

Comparing the percentage sensitivities of the sensor for both the conductance and capacitance response we can see that the values obtained for capacitance response is higher than the conductance response. This can be attributed to the possibility of an additional change in dielectric constant along with the change in conductivity. Therefore the capacitance response obtained due to secondary effects of the conductance, along with a change in dielectric constant results in better sensitivities for capacitance response than the conductance response.

Table 4.1 Device structure, growth conditions and their results

Device	**Structure/Growth conditions**	**Result**
Srk_1 to srk_4	Bus bars on AAO with CNTs embedded in it	No response
Srk_4 to srk_8	Bus bars on spin coated CNTs suspended in DMF	No response
Srk_8,srk_9_srk_10	Bus bars on dip coated CNTs suspended in DMF	No response
Srk_11,srk_12	DEP on IDE electrodes at 10V 1MhZ	No response
Srk_13 to srk_26	CNTs grown via CVD at 800^0 C with varying growth times(8 to 15min)	CNT growth all over electrodes
Srk_27	CNT growth on Titanium electrodes	CNT growth all over electrodes
Srk_28 to srk_40	CNT grown via CVD at 750^0 C for various growth times (3 to 15 min)	Excellent growth confinement with good response

From Table 4.1 we can see that almost all the devices with CNTs grown at 800^0 C have not achieved growth confinement. However CVD temperature of 750^0 C supported the growth confinement of CNTs. Quality of gold film deposited plays a very important role

in determining the extent of growth confinement achieved. Minute degradation of the film quality results in carbon nanotube growth even on the electrodes. Three devices were fabricated using the same CNT growth condition (750^{o} C for 6minutes) and sensitivities for conductance response were found to be 11.17, 20.23 and 8.7 percent respectively. The sensitivities for capacitance response were found to be 18.49, 28.13 and 14.3 percent respectively. These differences in sensitivities can be explained by the inconsistency in amorphous carbon layer formation. CVD process is initiated once the vapors of ferrocene xylene mixture are observed at the other end of the tube. These vapors are observed usually in between 2 to 3 minutes with no control over the time. This causes huge differences in the morphology of amorphous carbon layers formed over the CNTs, that in turn has an effect on the sensitivities However high sensitivities of about >10 percent has been achieved for growth times in range of 3~10minutes, which are of significant value with respect to the devices mentioned in section 1.4.

4.3. Mathematical Model Results

For the sensor discussed above the conductance measured between the electrodes is 0.06058 Siemens which can be substituted in equation (3) as below.

$$G_{Total} = \{G_{L-X} + G_d\}(N-1)$$

Which implies

$$0.06058 = \{G_{L-X} + G_d\}(N-1)$$

Which further reduces to

$$0.06058 = \sigma H(N-1)\{\frac{(L-X)}{d} + \frac{d}{(L+X)}\}$$

Substituting the values of N=5, H= 50*10^{-6} m, L= ½ ", X=d= 1/16" in the above equation we get

$$\sigma = 42.59\, S.m^{-1}$$

The capacitance measured between the electrodes of the sensor discussed above is 1.498 nF. Using an estimated value of $\varepsilon = 4\varepsilon_0$ value in equation (3) we have

$$C_{total} = \{C_{L-X} + C_d\}(N-1)$$

which reduces to

$$C_{total} = \varepsilon h(N-1)\{\frac{(L-X)}{d} + \frac{d}{(L+X)}\}$$

Using $\varepsilon = 4\varepsilon_0$ where ε_0 = 8.85 * 10^{-12} F.m^{-1} , h = 1 * 10^{-6} m

we get C_{total} = 1.06 * 10^{-15} F

which is not in comparable terms to the measured value. Only a very large value of ε_r (order of 10^5) can satisfy the model to fit to the measured value. The other theory which

can support this capacitance is a very small value of the denominators in equations (3) and (4).

Assuming a denominator D in both equations (3) and (4) we have

$$C_{total} = \varepsilon h(N-1)\{\frac{(L-X)}{D} + \frac{d}{D}\} \qquad (11)$$

If we use $\varepsilon = 4\varepsilon_0$ in the above equation, to get a capacitance of 1.5 nF, 'D' must have a value of 119.88 nm. Capacitance due to such a short value of 'D' can arise only due to junction capacitance of a diode. Therefore we can model our device with two back to back schottky diodes separated by a MWCNT resistive layer. These schottky diodes are present at the metal semiconductor interface. The depletion layer in the CNT matrix might be responsible for this junction capacitance. Figure 4.15 shows the equivalent circuit for this model.

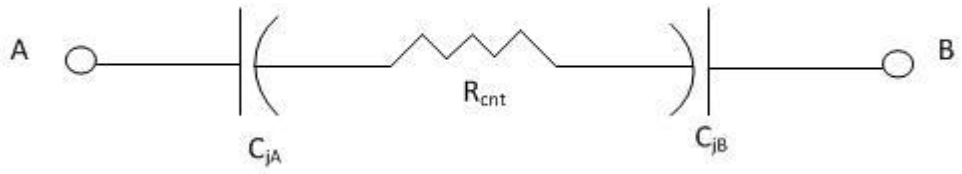

Figure 4.15: Equivalent circuit for the back to back diode model

Figure 4.16 shows the V-I characteristics of a sensor device. The plot clearly shows a nonlinear behavior for the electrode-graphite contact (graphite paste applied on CNTs serve as an ohmic contact).

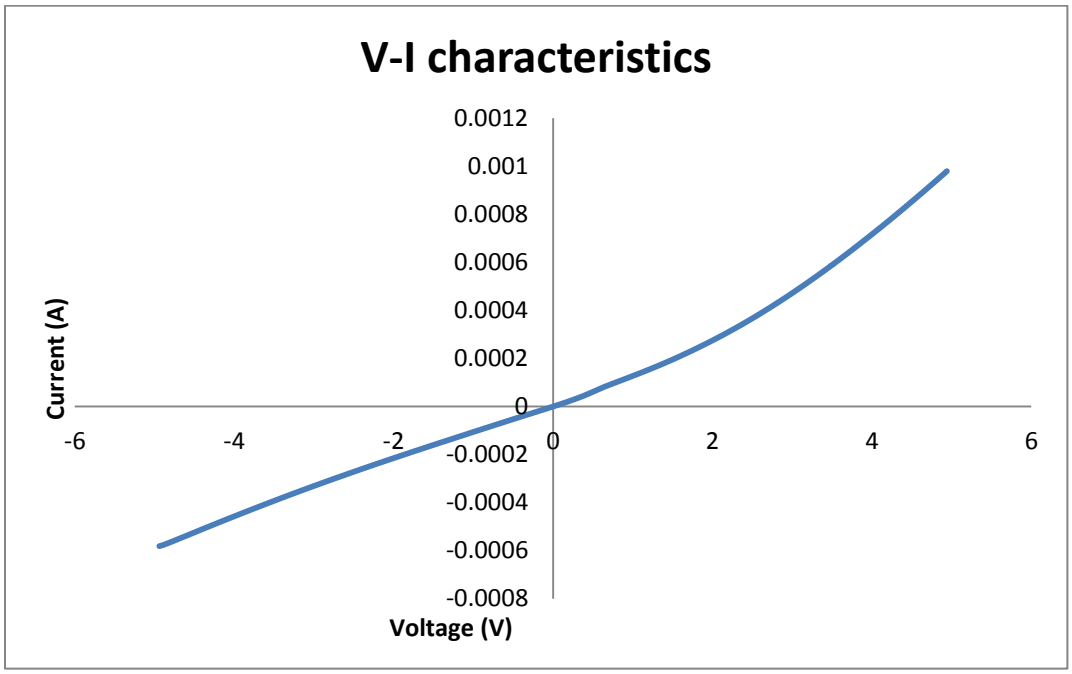

Figure 4.16: Diode behavior of a sensor for the contacts. This device can be modeled as a diode with a shunt resistance.

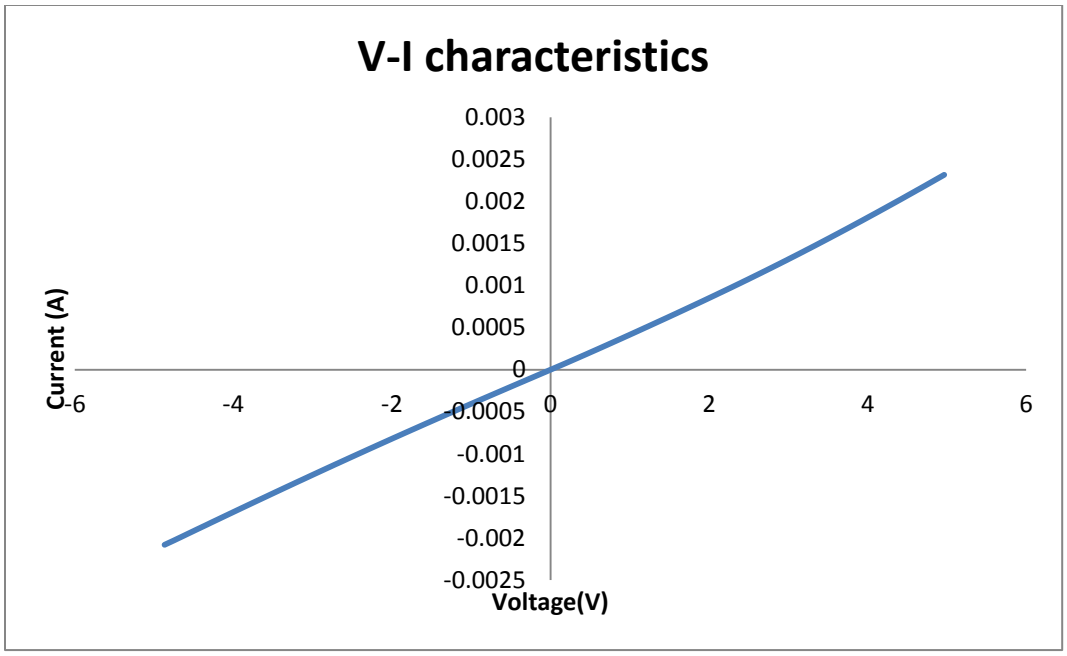

Figure 4.17: Ohmic behavior of the sensor for the electrode- CNT contact.

Figure 4.17 shows the V-I characteristics of another device fabricated with similar growth conditions. This ohmic behavior might be due to barrier tunneling. Typically gold makes an ohmic contact with most of the semiconductors. However the phenomenon of Fermi pinning might be the possible reason for the schottky behavior. If a high number of surface states are present on the nanotube (because of the dangling bonds on the surface), these states act as charge traps which pull the charges from the bulk material, thus forming a depletion layer pushing the fermi level down. This makes the metal semiconductor interface a schottky contact irrespective of the metal work function.

5. Conclusions and Suggestions for future work:

Multi walled carbon nanotube growth confinement has been achieved on Au patterned SiO_2 substrates to a large extent. A device structure was conceived to exploit this technique to build a capacitance based gas sensor. A sensor was successfully built to achieve the desired device structure with the carbon nanotubes grown in between the electrodes. However due to highly conductive amorphous carbon layer formed on the carbon nanotubes during the CVD growth, the device was found to be a conductive sensor. The capacitance and the conductance response of the device to 100 ppm of NO_2 gas exposure were studied. A cumulative response of 27.97% and 20.01% has been achieved for capacitance and conductance response respectively. The sensitivity obtained for capacitance response was higher than the conductance response.

A lot of potential is present for the capacitive sensor because of its wireless monitoring capabilities. This can be particularly useful in the case of gas sensing from a sealed chamber. Also because of the expensive gold electrodes being used in fabrication, the thickness of the electrodes was limited to only 1 micron. The carbon nanotubes grown in between the electrodes however were about 50 microns in size. Increasing the height of the gold electrodes might significantly improve the capacitance response of the sensor due to more number of field lines passing through the tubes. Since gold is a fairly expensive material to use, research has to be done to find alternate metals which have a similar growth prohibiting effect on carbon nanotubes. Also getting rid of amorphous carbon layer through oxidation techniques might lead to a less conductive dielectric between the electrodes, resulting in a device with a dominating capacitance behavior. This will also fairly improve the mathematical fit in the discussed model.

References

1. Z.M Rittersma, "Recent achievements in miniaturised humidity sensors—a review of transduction techniques", 2002, *Sensors and actuators*, vol.96, pp. 196-210.

2.E.Traversa**,** "Ceramic sensors for humidity detection: the state-of-the-art and future developments"**,** 1995, *Sensors and actuators*, vol.23, pp.135-156.

3. R.Fenner,E.Zdankiewicz, "Micromachined water vapor sensors: a review of sensing technologies", 2002, *IEEE Sensors Journal*, vol.1 pp.309-317.

4. E.S.Snow,"Chemical Detection with a Single-Walled Nanotube capacitor",*2005 Science*,vol. 307 , pp. 1942-1945.

5. K.Ong, K.Zheng, C.A. Grimes, "A Wireless, Passive Carbon Nanotube-Based gas sensor", 2002, IEEE Sensors Journal, vol.2, pp.82-88.

6. S. Chopra, K. McGuire, N. Gothard, A. M. Rao, A. Pham, "Selective gas detection using a carbon nanotube sensor", 2003, *Applied Physics Letters*, vol.83, pp.2280-2282.

7. S. Chopra, A. Pham, J. Gaillard, A. Parker, A. M. Rao, "Carbon-nanotube-based resonant-circuit sensor for ammonia", *2002, Applied Physics Letters*, vol. 80, pp.4632-4634.

8. J. Suehiro, G. Zhou, M Hara, " Fabrication of a carbon nanotube-based gas sensor using dielectrophoresis and itsapplication for ammonia detection by impedance spectroscopy", *2003, Joumal of Physics*, vol. 36, pp. L109-114.

9. J.T.W. Yeow, J.P.M.She, "Carbon nanotube-enhanced capillary condensation for a capacitive humidity sensor", 2007, *Nanotechnology*, vol.17, pp.5441-5448.

10. Y.Chen, F. Meng, M Li, J. Liu**,** "Novel capacitive sensor: Fabrication from carbon nanotube arrays and sensing", 2009, *Sensors and Actuators*, vol.140, pp. 396-401.

11. S.IIjima, "Helical microtubules of graphitic carbon", 1991, *Nature*, vol.354, pp. 56-58.

12. R. Saito, G. Dresselhaus, M. S. Dresselhaus, "Physical Properties of Carbon Nanotubes", 1998, pp. 14.

13. M. S. Dresselhaus, G. Dresselhaus, and P. C. Eklund**,** " Science of Fullerenes and Carbon Nanotubes", 1996, *Academic press.*

14. The University of Reading Website,2010,"A carbon nanotube page". Available at "http://www.personal.reading.ac.uk/~scsharip/tubes.htm".

15. S. Peng and K. Cho "Chemical control of nanotube electronics*","00,Nanotechnology* vol.11, pp-57-60.

16. J. Zhao, A. Buldum, J. Han, and J. P. Lu," Gas molecule adsorption in carbon nanotubes and nanotube bundles", 2002, *Nanotechnology*, vol.13, pp. 195-200.

17. C. Cantalini, L. Valentini, L. Lozzi, I. Armentano, J. M. Kenny, "NO2 gas sensitivity of carbon nanotubes obtained by plasma enhanced chemical vapor deposition",2003, *Sensors and Actuators*, vol.93, pp.333-337.

18. P. G. Collins, K. Bradley, M. Ishigami, and A. Zettl, "Extreme oxygen sensitivity of electronic properties of carbon nanotubes", 2000, *Science*,vol-287, pp.1801-1804

19. S.H. Jhi, S. G. Louie, and M. L. Cohen, "Electronic properties of oxidized carbon nanotubes", 2000, *Phys rev lett.*, vol.85, pp.1710-3.

20. R Langlet, M Arab, F Picaud, "Influence of molecular adsorption on the dielectric properties of a single wall nanotube: A model sensor", 2004, *J. Chem. Phys.*,vol. 121, pp.9655-9665.

21. A.Cao, X Zhang, C Xu, J Liang, D Wu, B Wei, "Synthesis of well-aligned carbon nanotube network on a gold-patterned quartz substrate", 2001, *Appl.Surface Science*,vol.181, pp. 234-238.

22. T.Guo, P. Nicolaev, A. Thess, D. T. Colbert,R. E. Smalley, " Catalytic growth of single-walled nanotubes by laser vaporization",1995, *Chem. Phys. Lett*., vol. 243, pp. 49-54 .

23.W.Z Li, "Large-Scale Synthesis of Aligned Carbon Nanotubes**",** 1996, *Science* ,vol.274, pp.1701-1703.

24.R.T.K. Baker, P.S. Harris, "Formation of filamentous carbon from iron, cobalt and chromium catalyzed decomposition of acetylene", 1973, *Journal of Catalysis*, vol.30, pp. 86-95.

25. R.T.K Baker, "Catalytic growth of carbon filaments", 1989, *Carbon*, vol.27, pp.315-323.

26. F.J. Derbyshire, A.E.B. Presland and D.L. Trimm**,** " Graphite formation by the dissolution-precipitation of carbon in cobalt, nickel and iron", 1975, *Carbon*, vol.13, pp.111-113.

27. S. B. Sinnott, R. Andrews, D. Qian, A. M. Rao, Z. Mao, E. C. Dickey and F. Derbyshire," Model of carbon nanotube growth through chemical vapor deposition",1999, *Chem Phys Lett***,** vol. 315. pp.25-30.

28. S.Huang, A.W.H Mau, "Selective Growth of Aligned Carbon Nanotubes on a Silver Patterned Substrate by the Silver Mirror Reaction", 2003, *J. Phys. Chem. B,* vol.107, pp.3455-3458.

29. W. Kern, D.A Puotinen," Cleaning solutions based on hydorogen peroxide for use in silicon semiconductor technology", 1970, *RCA Rev,*vol.31 pp.187-206.

30. R.Andrews, D. Jacques, D.Qian, T. Rantell." Multiwall Carbon Nanotubes: Synthesis and Application", 2002, *Acc. Chem. Res,*vol.35, pp. 1008–1017.

31.R.Vajtai et al.,"Building and testing organized architectures of carbon nanotubes", 2004, *IEEE Transactions on Nanotechnology,* vol.2, pp.355-361.

32. R.Mangu, S.Rajaputra, P.Clore,D.Qian, R.Andrews,V.P.Singh ,"Ammonia sensing properties of multiwalled carbon nanotubes embedded in porous alumina templates", 2008, *Material Science Engg,* vol.174, pp.2-8.

Vita

Srikanth Durgamahanty was born in Vizag, Andhra Pradesh, India on May 15, 1987. After completing Bachelor of Technology in Electronics and Instrumentation Engineering from Andhra University, Vizag, India, in 2008, he enrolled for Master's Program in Electrical Engineering at the University of Kentucky in Fall 2008. He, during his Master's program, worked as a researcher in the field of nanotechnology and developed carbon nanotube sensors for gas detection.